A deep level transient spectroscopic study of boron-ion-implanted $Si_{1-x}Ge_x/Si$ single quantum wells

1997 J. Phys.: Condens. Matter 9 3427

(http://iopscience.iop.org/0953-8984/9/16/014)

J. Phys.: Condens. Matter **9** (1997) 3427–3433. Printed in the UK PII: S0953-8984(97)70670-2

A deep level transient spectroscopic study of boron-ion-implanted $Si_{1-x}Ge_x/Si$ single quantum wells

Fang Lu, Jianbao Wang, Jiayu Jiang, Dawei Gong, Henghui Sun and Xun Wang

Surface Physics Laboratory and Fudan T D Lee Physics Laboratory, Fudan University, Shanghai, 200433, People's Republic of China

Received 4 January 1996, in final form 31 July 1996

Abstract. The defects induced by boron-ion implantation with a relatively low dosage of 1×10^{12} cm^{-2} in $Si_{1-x}Ge_x/Si$ single quantum wells are studied by deep level transient spectroscopy (DLTS). For low Ge content x, a defect level H_2 at an energy of 0.52 eV above the silicon valence band edge was found in the well region and its boundaries. For samples with higher Ge content, such that the strain is released, an electron trap E_2 rather than H_2 is formed by the ion implantation. Rapid thermal annealing at 600 °C removes most of the H_2 defects induced by the ion implantation without changing the properties of the quantum well.

Ion implantation is a standard semiconductor device technology and is likely to be beneficially employed in fabricating $Si_{1-x}Ge_x/Si$ heterostructure devices. In order to benefit from this technique the effects of ion implantation and post-implantation thermal annealing on the crystalline structures should be understood. In previous work various structural characterization techniques, such as Rutherford backscattering spectrometry, transmission electron microscopy and x-ray double-crystal diffractometry, have been used to study the damage and strain in epitaxial $Si_{1-x}Ge_x$ alloy layers induced by ion implantation and the relationship of stress to the crystalline regrowth process during the post-implantation thermal annealing treatment [1–5]. However, for $Si_{1-x}Ge_x/Si$ quantum wells, work on studying the creation and elimination of defects induced by the ion implantation and post-implantation thermal annealing has not been reported yet. In this work, we have investigated defects in boron-ion-implanted $Si_{1-x}Ge_x/Si$ single quantum well samples by using deep level transient spectroscopy (DLTS). The results show that the defects created by boron-ion implantation are related to the built-in strain in the quantum well structure. Rapid thermal annealing (RTA) at 1000 °C after the ion implantation fully removed the residual defects.

The samples used in this study were grown by molecular beam epitaxy at a temperature of 500 °C on p-type Si(100) substrates with a hole concentration of 2×10^{18} cm^{-3}. The $Si_{1-x}Ge_x$ well layer is sandwiched between a Si buffer layer 300–500 nm thick and a Si cap layer of thickness 300 nm. The structural parameters for different quantum well samples are listed in table 1. The unintentionally doped Si buffer, Si cap and $Si_{1-x}Ge_x$ epilayers were found to be p-type with a doping concentration of about 1×10^{16} cm^{-3}. The boron-ion implantation was performed at an energy of 40 keV and a dosage of 1×10^{12} cm^{-2}. From the computer simulation the peak boron concentration is estimated to be 9×10^{16} cm^{-3} and is located near the centre of the cap layer, the full width at half maximum of the

0953-8984/97/163427+07$19.50

boron distribution being about 45 mn. So the implanted ions are basically constrained to be within the cap layer and do not reach the quantum well region. Because of the low dose, it was found [1] that the cap layer still remains in the crystalline form after the implantation. Thus it is possible to measure DLTS signals after the implantation without post-implantation annealing. The sample was fabricated into a testing structure. An ohmic contact was made on the back side by evaporating Al followed by alloying in N_2 ambient at 500 °C and a Schottky contact was formed on the top of the cap layer by evaporating Al through a mask without alloying. The diameter of the Schottky electrode is about 0.8 mm.

Table 1. Structural parameters of quantum well samples.

	Samples			
	S_1	S_2	S_3	S_4
Well width L_w (nm)	15	15	15	3
Ge composition (x)	0.33	0.40	0.53	0.33
h_c^t (nm)[a]	5.5	4.5	2.7	5.5
h_c^e (nm)[b]	30	20	7	30

[a] According to the theory of Matthews and Blackeslee [8].
[b] The critical thickness according to Bean *et al* [9].

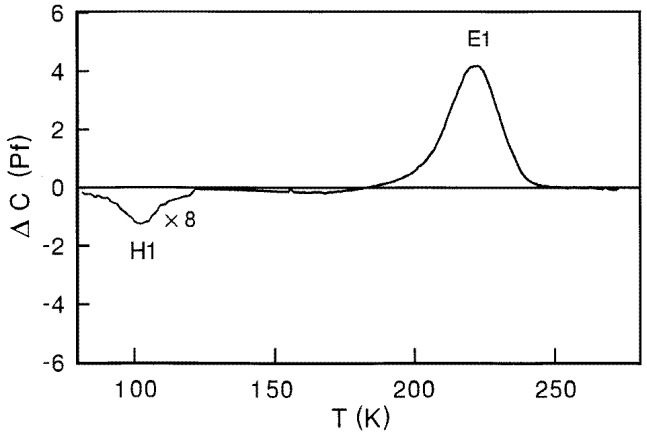

Figure 1. The DLTS spectrum of unimplanted sample S_1; measured at $V_R = -2$ V and $V_p = 3$ V.

The DLTS spectrum of unimplanted sample S_1 measured at a reverse bias V_R of -2 V and with an injection pulse amplitude V_p of 3 V is shown in figure 1 in which two peaks labelled H_1 and E_1 can be clearly seen. Peak H_1 is a majority carrier peak which originates from the hole emission from the well to the barrier region [6], since the quantum well could be seen as a 'big trap' which acts just like a deep level trap in terms of carrier emission and capture. According to the thermal emission model of Debbar *et al* [7], the activation energy of peak H_1 which is deemed as the energy difference between the hole ground state in the well and the Si barrier is determined from the DLTS to be 0.23 eV which is very close to the predicted valence band offset of 0.24 eV. It is reasonable since the well width of the sample S_1 is 15 nm so the hole ground state is almost equal to the valence band

edge of the $Si_{1-x}Ge_x$ well. This coincidence verifies that the assignment of H_1 to the well emission is correct. The existence of peak H_1 is indicative of the good crystalline quality of the sample, otherwise the carrier emission from the well would have been smeared out by the emission from other defects or by the leakage current. Peak E_1 is a minority carrier peak which is not observable in the ordinary DLTS measurement of a p-type Schottky diode structure. The origin of this minority carrier peak has been discussed in our previous work [6, 8]. Suppose that there exist donor-like defects at the interface of a p-type heterojunction, then the quasi-Fermi level of electrons will be pinned near the defect level if the defect density is relatively large. Figure 2 is the energy band diagram which shows the relative positions of the conduction band and valence band edges E_c and E_v the defect levels E_1 and quasi-Fermi levels E_{Fn} and E_{Fp} under a reverse bias voltage. When the bias voltage changes a small variation in the Fermi level will lead to a great change in the electron population in the defect level and thus a reduction in the number of negative charges in the space-charge region. In order to maintain electrical neutralization, the space-charge region is thus expanded, leading to a decrease in capacitance and giving rise to a minority carrier peak in the DLTS measurement. Except for the interfacial defects the original sample S_1 is free of other defects, as shown in figure 1.

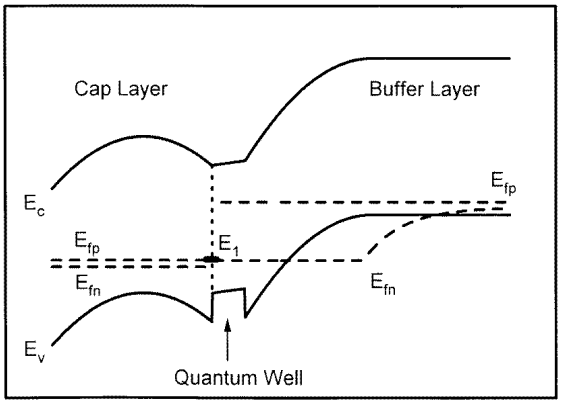

Figure 2. A schematic band diagram of a reverse-biased Schottky diode with a single quantum well in the depletion region.

The DLTS spectra of a series of implanted samples S_1, S_2, S_3 and S_4 are shown in figures 3 and 4. The well emission signal is remarkably reduced. Instead a new majority carrier peak H_2, attributed to a defect level induced by the ion implantation, was seen in DLTS. The energy level of defect H_2 is determined to be $E_v + 0.52$ eV, where E_v is the valence band edge of Si. The ratio of the peak height ΔC to the steady state capacitance C in DLTS is proportional to the apparent defect density of H_2. From figure 3 it could be seen that the densities of defect H_2 are different depending on the Ge composition in the well, but the peak temperatures, namely the energies of the defect levels are the same. On the other hand it can be seen from figure 4 that the defect density of H_2 is almost independent of the well width if the Ge compositions in the wells are the same.

Before giving an analysis of the relation between the defect density of H_2 and the well structure, let us first investigate the depth distribution of the defect H_2. By changing the bias voltage, the space-charge region of the Schottky barrier would extend over the cap and the quantum well. The DLTS spectra of sample S_1 measured at different bias voltages are shown

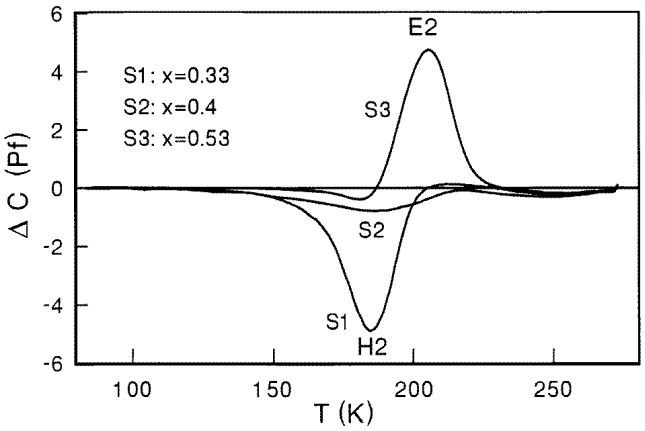

Figure 3. DLTS spectra of samples S_1, S_2 and S_3 measured at $V_R = -2$ V and $V_P = 3$ V.

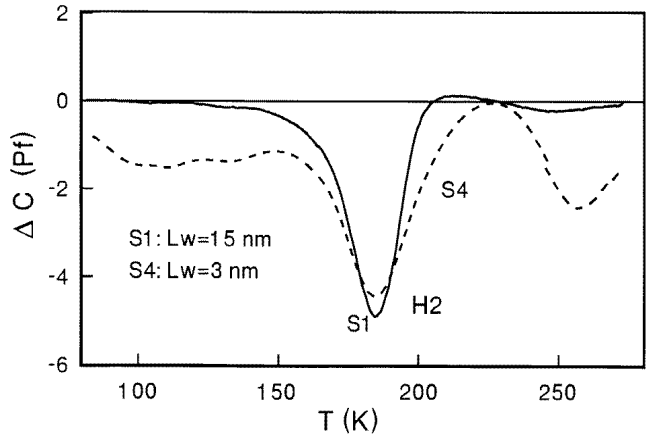

Figure 4. DLTS spectra of samples S_1 (full curve) and S_4, (broken curve) measured at $V_R = -2$ V and $V_P = 3$ V.

in figure 5. From the capacitance–voltage measurements and the numerical simulation (not shown here), the boundary of the space-charge region at zero bias is expected near the well boundary. Due to the carrier accumulation in the quantum well the boundary of the space-charge region is basically pinned within the well region as the bias voltage varies from -0.5 to -2.0 V. At the bias voltage of -2.5 V, the holes in the quantum well are depleted and the space-charge region is extended into the buffer layer. The DLTS peaks in figure 5 are thus related to the defects distributed basically in the well region. The monotonic increase in peak height with bias voltage from -0.5 to -2.0 V is consistent with the above assignment. In order to determine the defect distribution further, the surface of S_1 was etched by anodic oxidation and HF step by step after boron-ion implantation. Table 2 shows the experimental values of $\Delta C/C$ after etching away different layer thicknesses. The defect density does not change even after more than half of the cap layer has been removed, but disappears fully in DLTS if the cap layer and the quantum well have been etched away completely. This means that there is no defect in the buffer and the substrate. This again supports the

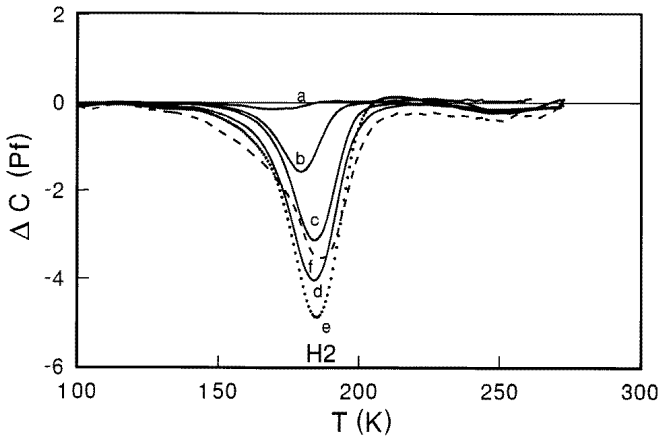

Figure 5. The dependence of the majority carrier peak H_2 of sample S_1 on V_R and V_P: (*a*) $V_R = 0$ V, $V_P = 1$ V; (*b*) $V_R = 0.5$ V, $V_p = 1.5$ V; (*c*) $V_R = -1.0$ V, $V_P = 2.0$ V; (*d*) $V_R = -1.5$ V, $V_P = 2.5$ V; (*e*) $V_R = -2.0$ V, $V_P = 3.0$ V and (*f*) $V_R = -2.5$ V, $V_P = 3.5$ V.

Table 2. $\Delta C/C$ of defect H_2 after etching away different layer thicknesses.

	Thickness removal (nm)			
	0	90	180	360
ΔC (pF)	4.89	7.43	2.77	0
C (pF)	130	210	74	80
$\Delta C/C$	0.037	0.035	0.037	0

hypothesis that the measured defects induced by ion implantation are mostly distributed in the well region, including its boundary areas. It is not known whether there exists a defect in the cap layer which is included in the space-charge region of the Schottky barrier even at zero bias.

The defect H_2 occurs in the quantum well region which the implanted ions do not reach, as described previously. The origin of the defect H_2 in the unimplanted well region seems to be due to the interaction between the ion-implantation-induced damage and the misfit strain in the quantum well. The fact that the defect densities of H_2 are different for samples with different Ge contents implies that the defect is related to the magnitude of the built-in strain. In samples S_1, S_2 and S_3, the misfit strains are different. The lattice mismatches of quantum wells are 0.014, 0.017 and 0.022 for samples S_1, S_2 and S_3, respectively; the critical thicknesses for pseudomorphic growth of these three samples are different. Listed in table 1 are the critical thicknesses h_c^t predicted theoretically by Matthews and Blakeslee based on the mechanical equilibrium model [9] and the experimental values h_c^e found by Bean *et al* [10]. For sample S_3, the layer thickness of the quantum well is larger than both h_c^e and h_c^t, therefore the strain is expected to be fully relaxed. The well thickness of sample S_1 is well below h_c^e, so the strain is expected to be the largest among those of these three samples. For sample S_2, the well thickness is close to h_c^e, so it is suggested that the strain is partially relaxed. This argument is supported by our admittance spectroscopic measurements of the valence band offset ΔE_v. The measured ΔE_v of sample S_1 (without implantation) is quite close to the theoretically predicted value of a pseudomorphically

grown $Si_{1-x}Ge_x/Si$ heterojunction, whilst for samples S_2 and S_3 (without implantation) the experimental ΔE_v deviates from the theoretically predicted one which resulted from strain relaxation. Since the strains in samples S_2 and S_3 are partially or fully relaxed, the low-dose boron-ion implantation does not induce an H_2 defect. Instead, another minority carrier peak E_2 appears in figure 3 for sample S_3. Also, the significant reduction and disappearance of the H_2 peak in samples S_2 and S_3 compared with sample S_1 illustrate that the defect H_2 induced by ion implantation is related to the built-in strain in the quantum well.

To remove the ion-implantation-induced defects, rapid thermal annealing (RTA) was performed on sample S_1 at the temperatures of 400, 600, 800 and 1000 °C for 10 s in nitrogen ambient. The DLTS spectra after RTA are shown in figure 6. The defect peak H_2 is greatly suppressed after RTA at 600 °C and vanishes after RTA at 1000 °C. However, the high-temperature treatment causes strain relaxation and interfacial atomic intermixing in the quantum well. In this work we measured the DLTS of sample S_1 (without ion implantation) after RTA treatments and determined the valence band offsets from the well emission peak H_1. The results show that ΔE_v varies with the annealing temperature: 0.24 eV for 400 °C, 0.22 eV for 600 °C and 0.21 eV for 800 °C. After RTA at 1000 °C, peak H_1 is no longer visible so that the band offset cannot be determined from DLTS. The change in ΔE_v after RTA is indicative of the strain relaxation. This result is the same as that of [11]. Our admittance spectroscopic measurements showed that the valence band offset of sample S_1 after implantation remains unchanged if the RTA temperature is no higher than 600 °C. For the quantum well sample processed with ion implantation it seems that the annealing temperature of 600 °C is appropriate not only for removing most of the defects induced by the implantation but also to avoid strain relaxation.

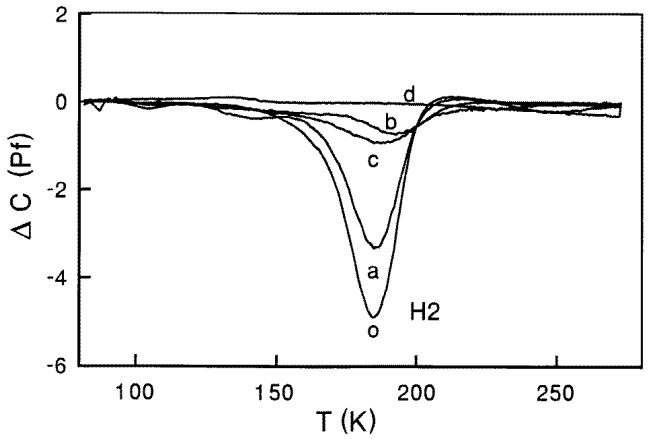

Figure 6. DLTS spectra of sample S_1 after RTA at different temperatures. (○) no annealing, (*a*) 400 °C, (*b*) 600 °C, (*c*) 800 °C and (*d*) 1000 °C.

In conclusion, by using DLTS measurements, it has been found that low-dose boron-ion implantation in the cap region of the $Si_{1-x}Ge_x/Si$ single quantum well will induce an acceptor-like defect level in the well region at an energy of 0.52 eV above the silicon valence band edge. This defect level is generated by the interaction between the implantation-induced lattice distortion and the built-in strain, so its concentration is closely related to the strain. For the sample in which the strain is relaxed, the acceptor-like defect is not visible in the DLTS spectrum, instead an electron trap level is formed as a result of ion

implantation. After treating the sample by RTA at 600 °C, most of the ion-implantation-induced defects could be removed while the interfaces of the quantum well still keep the pseudomorphic form. To remove the defects induced by ion implantation fully, the RTA should be performed at 1000 °C but the strain in the quantum well will be relaxed by such a high-temperature treatment.

Acknowledgments

This work was partially supported by the National Natural Science Foundation of the People's Republic of China and the Ion Beam Laboratory, Shanghai Institute of Metallurgy, Chinese Academy of Sciences.

References

[1] Hull R, Bean J C, Bonar J M, Higashi G S, Short K T, Temkin H and White E 1990 *Appl. Phys. Lett.* **56** 2445
[2] Haynes T E and Holland O W 1992 *Appl. Phys. Lett.* **61** 61
[3] Lie D Y C, Vantomme A, Eisen F, Vreeland T Jr, Nicolet M-A, Carns T K, Arbet-Engles V and Wang K L 1993 *J. Appl. Phys.* **74** 6039
[4] Hong Q Z, Zhu J G, Mayer J W, Xia W and Lau S S 1992 *J. Appl. Phys.* **71** 1768
[5] Hong S Q, Hong Q Z, Zhu J G and Mayer J W 1993 *Appl. Phys. Lett.* **63** 2053
[6] Wang Q H, Lu F, Gong D W, Wang J B, Sun H H and Wang X 1994 *Phys. Rev.* B **50** 18 226
[7] Debbar N, Biswas D and Bhattacharya P 1989 *Phys. Rev.* B **40** 1058
[8] Lu F, Gong D, Sun H and Wang X 1995 *J. Appl. Phys.* **77** 213
[9] Matthews J W and Blakeslee A E 1974 *J. Cryst. Growth* **27** 118
[10] Bean J C, Feldman L C, Fiory A T, Nakahara S and Robinson I K 1984 *J. Vac. Sci. Technol.* A **2** 436
[11] Zhou G L, Zhang X J, Sheng C and Wang X 1993 *J. Cryst. Growth* **127** 456